Separation and Purification Technology, Volume 201, 7 August 2018, pp. 139-147
DOI:10.1016/j.seppur.2018.03.003

Determining how polymer-bubble interactions impact algal separation using the novel "Posi"-dissolved air flotation process

Narasinga Rao Hanumanth Rao,[a, b] Anthony M. Granville,[b, c] Christine I. Browne,[d, e] Raymond R. Dagastine,[d, e] Russell Yap,[a, f] Bruce Jefferson,[g] Rita K. Henderson [a, *]

[a] *Microbial Advanced Separation Systems Laboratory (bioMASS Lab), School of Chemical Engineering, The University of New South Wales, Sydney, NSW 2052, Australia*

[b] *Centre for Advanced Macromolecular Design (CAMD), School of Chemical Engineering, The University of New South Wales, Sydney, NSW 2052, Australia*

[c] *TDK Research Solutions, Bondi Junction, NSW 2022, Australia (Present address)*

[d] *Department of Chemical Engineering, The University of Melbourne, Parkville, Victoria 3010, Australia*

[e] *Particulate Fluids Processing Centre, The University of Melbourne, Parkville, Victoria 3010, Australia*

[f] *BASF Corp. Charlotte, North Carolina 28273, USA (Present address)*

[g] *Cranfield Water Science Institute, School of Applied Sciences, Cranfield University, Bedfordshire MK43 0AL, UK*

***** Corresponding author - r.henderson@unsw.edu.au

ABSTRACT: The novel dissolved air flotation (DAF) process that uses hydrophobically-modified polymers (HMPs) to generate positively charged bubbles (PosiDAF) has been shown to

separate negatively charged algal cells without the need for coagulation-flocculation. Previous research has been limited to HMPs of poly(N,N-dimethylaminoethyl methacrylate) (PDMAEMA) and, while they were effective at bench-scale, performance at pilot-scale was better using commercial poly(N,N-diallyl-N,N-dimethylammonium chloride) (PDADMAC). Hence, the aim of this research was to compare the effectiveness of PDADMAC modified with aliphatic and aromatic moieties in comparison to previously tested PDMAEMA HMPs in respect to algal cell separation and minimisation of effluent polymer concentration, as well as defining the underlying polymer-bubble interaction mechanisms. Polymer-bubble adhesion properties were measured using atomic force microscopy (AFM) while polymer concentration was monitored via zeta potential and, where possible, assays using fluorescence spectroscopy. Both PDADMAC functionalised with a fluorinated aromatic group (PDADMAC-BCF) and PDMAEMA modified with 1-bromodecane respectively, gave effective cell separation, while the treated effluent zeta potential values at maximum cell removal were lower than the other polymers trialled. The effluent polymer concentration when using PDADMAC-BCF was four times lower in comparison to another aromatically modified PDADMAC polymer. AFM studies indicated that, in contrast to the PDMAEMA-based polymers, the PDADMAC-based polymers did not adsorb closely to the bubble surface. The different polymer-bubble interactions indicate that separation mechanisms will also vary, potentially leading to differences in process effectiveness when explored at pilot scale.

KEYWORDS: Algae harvesting; atomic force microscopy; gas-liquid interface; multiphase system; PosiDAF; water treatment.

Table of Notation

Abbreviation	Expansion
AFM	Atomic force microscopy
ANACC	Australian National Algae Culture Collection
AOM	Algal organic matter
CCAP	Culture Collection for Algae and Protozoa
CDW	Chan-Dagastine-White model
CSIRO	Commonwealth Scientific and Industrial Research Organisation
CV	*Chlorella vulgaris* CS-42/7
DAF	Dissolved air flotation
DMAEMA	2-(*N, N*-dimethylamino)ethyl methacrylate
F-EEM	Fluorescence excitation emission matrix
HLB	Hydrophile-lipophile balance
HMP	Hydrophobically modified polymer
MA555	*Microcystis aeruginosa* CS-555/1
MA564	*Microcystis aeruginosa* CS-564/01
M_w	Molecular weight
NMR	Nuclear magnetic resonance
PCD	Particle charge detector
PDADMAC	Poly(*N, N*-diallyl-*N,N*-dimethylammonium chloride)
PDADMAC-BC	PDADMAC quaternised with benzyl chloride
PDADMAC-BCF	PDADMAC quaternised with 4-fluoro benzyl chloride
PDADMAC-C4	PDADMAC quaternised with 1-chlorobutane
PDADMAC-C5	PDADMAC quaternised with 1-chloropentane
PDADMAC-C10	PDADMAC quaternised with 1-chlorodecane
PDMAEMA	Poly(*N, N*-dimethylaminoethyl methacrylate)
PDMAEMA-C10	PDMAEMA quaternised with 1-brompdecane

1. INTRODUCTION

Polymers are frequently used to aid floc formation in water treatment, prior to separation by either sedimentation or dissolved air flotation (DAF), in which flocs attach to anionic microbubbles and are floated from solution [1-7]. The surface modification of microbubbles generated in DAF via polymer addition to the saturator unit, in a novel process referred to as PosiDAF, has received attention as an alternative to traditional coagulation and flocculation of

influent particles [8-12]. The potential benefits include reduced chemical demand, removal of metal salt contamination from the float and consequent reduction in sludge volume and increased solid-liquid ratio of the float. In particular, conventional cationic polymers commonly handled at water treatment plants, including poly(*N*, *N*-diallyl-*N*,*N*-dimethylammonium chloride) (PDADMAC) and poly(*N*, *N*-dimethylaminoethyl methacrylate) (PDMAEMA), were used to produce positively charged bubble surfaces for the solid-liquid separation of algae [8, 13, 14]. Early PosiDAF investigations showed that separation effectiveness was comparable to that of the traditional process for certain microalgal species [8], thus demonstrating proof of concept for this new approach. However, challenges were observed including a positively charged effluent which indicated a significant concentration of polymer was present in the effluent [8], and a variation in process efficiency between different species [8]; the latter being a challenge that is also observed with conventional separation as well [15-19]. To combat these challenges, it was concluded that a review of polymer design was warranted as the polymers used had not been designed to modify bubble surfaces.

It was identified that increasing the surface activity of cationic water treatment polymers to encourage adhesion of the polymer to the bubble surface and minimise carryover to downstream processes had potential [14]. Consequently, an initial study saw the development of several PDMAEMA variants by modifying the base polymer to incorporate a range of aliphatic hydrophobic groups [14]. When these hydrophobically modified polymers (HMPs) were applied in PosiDAF on a bench scale, over 95% cell separation was achieved for a strain of *Microcystis aeruginosa* CS-564/01, while simultaneously maintaining a negatively charged effluent, suggesting a reduced effluent polymer concentration [14]. Interestingly, when trialled on a pilot scale and contrasted against commercially available PDADMAC, PDADMAC was found to

perform better than the HMPs of PDMAEMA, attributed in part to its enhanced positive charge [20, 21]. These outcomes indicate that further research into HMP generation using PDADMAC is necessary.

Recently, the functionalisation of PDADMAC with pendant hydrophobic groups to generate polymers with differing charge and structural characteristics was demonstrated [22]. Another study showed that when PDADMAC was modified with aromatic groups, the subsequent hydrophobicity facilitated bridging sheets of clay [23]. These outcomes demonstrate the potential for tailoring PDADMAC for application as a bubble modifier in PosiDAF. Hence, the current paper aims to develop a variety of HMPs of PDADMAC for PosiDAF application, including for the first time those incorporating aromatic groups, and contrast these against the performance of those previously generated using PDMAEMA [14].

The underlying mechanisms driving separation using PosiDAF remain unidentified. Separation effectiveness when using polymers as opposed to surfactants is much higher than can be modelled using the white water model [8, 24], indicating that complex interactions are involved. In previous studies, only limited information of the polymer-bubble interaction was reported via bubble charge measurements and surface tension [14] which limited elucidation of the mechanisms involved beyond confirming that HMPs of PDMAEMA were adhering at the bubble surface. Recently, atomic force microscopy (AFM) has been used to study structural forces between bubbles in polymer solutions such as sodium poly(styrene sulfonate) [25-27]. This suggests that the application of AFM to study polymer-bubble interactions in PosiDAF would help to better understand the PosiDAF process. Another gap in previous PosiDAF work has been the absence of a direct measure of polymer concentration in treated effluent. Until now, zeta potential measurements were employed to give an indirect indication of residual polymer. An

additional advantage of modifying PDADMAC with aromatic groups is the potential for quantifying polymer concentration in the effluent directly, through fluorescence measurements [28].

Hence, in the current study, a comparison of hydrophobically-modified PDMAEMA and PDADMAC based polymers, using both aromatic and aliphatic groups, was undertaken for PosiDAF, to separate one strain of *Chlorella vulgaris* CS-42/7 and two strains of *Microcystis aeruginosa* CS-564/01 and CS-555/1. Importantly, AFM was applied to quantify polymer-bubble interaction and, for select polymers, fluorescence measurements were employed to quantify the polymer concentration in treated effluent. In combining these measurements, the underlying process mechanisms leading to successful separation using PosiDAF were explored.

2. MATERIALS & METHODS

2.1 Chemicals

Unless otherwise stated, all chemicals were obtained from Sigma-Aldrich and used without any further purification. Low M_W (100,000 – 200,000 g/mol) poly(*N*, *N*-diallyl-*N*,*N*-dimethylammonium chloride) (PDADMAC, 20 wt% in H_2O) was lyophilised prior to use. Ethanolamine (Unilab, 97%), benzyl chloride (98%), 4-fluoro benzyl chloride (98%), 1-chlorobutane (98%), 1-chloropentane (97%), 1-chlorodecane (98%), 1-bromodecane (98%) were all used as received. 2-(N,N-dimethylamino)ethyl methacrylate (DMAEMA, Aldrich, 98%) was passed through a basic alumina column to remove inhibitor prior to use. 2,2'-Azobisisobutyronitrile (AIBN, Wako Chemicals, 98%) was re-crystallised twice from methanol.

2.2 Algae and cyanobacteria

Chlorella vulgaris (strain CS-42/7) and *Microcystis aeruginosa* (strains CS-555/1 and CS-564/01) were obtained from the Commonwealth Scientific and Industrial Research Organisation (CSIRO) Australian National Algae Culture Collection (ANACC), Hobart, Australia, and re-cultured in Jaworski [29] and MLA media [30], respectively. The cultures were subjected to a 16/8 h light/dark cycle, with an associated temperature control of 21 °C/ 15 °C, in 500 L, PG-50 and PG-120 cycling incubators (Labec, Australia) with a photosynthetic photon flux output of approximately 600 μmol/m^2s. These cultures were grown in several 250 mL conical flasks in batches of 100 mL. At the end of the exponential growth phase and upon the onset of the stationary growth phase (10-13 d), as determined by cell counting *via* light microscope (Leica DM750 Microscope, Switzerland) and a haemocytometer, the cells were harvested for jar testing.

2.3 Experimental methods

2.3.1 Synthesis of hydrophobically functionalised PDADMAC

The synthesis of hydrophobically functionalised PDADMAC was carried out in a two-step de-methylation and quaternisation of the polymer. The de-methylation of PDADMAC was carried out in the same manner as de-methylation of chiral [3, 22]-ionenes by generating the corresponding tertiary polyamine [31]. Briefly, 5 g of the lyophilised PDADMAC was reacted with 20 mL of ethanolamine in a round bottom flask equipped with a reflux condenser. The reaction mixture was heated to 165 °C for 4 h after which it was cooled to room temperature and mixed with 80 mL DI water. The resulting mixture was extracted thrice with 80 mL chloroform and any remaining water was stripped with anhydrous $MgSO_4$. Chloroform was removed under reduced pressure resulting in a waxy-yellow solid which was later characterised by ^{1}H NMR. The reaction scheme is described in Figure 1.

The quaternisation of the selectively de-methylated PDADMAC was carried out in the presence of n-alkyl halides [22] (Figure 1). In this study, the polymer and the respective alkyl chloride were mixed in a 1:1.2 molar ratio of the monomer units and heated to 65 °C for 96 - 120 h in the presence of chloroform. The solvent was then extracted under reduced pressure and the solids were dried in a vacuum oven for 24 h. The solids were dissolved in a 50:50 ethanol-water mixture and filtered using a UF membrane (MWCO 1000). The polyelectrolyte was lyophilised and analysed by ^{1}H NMR.

The following PDADMAC based polymers quaternised with aliphatic and aromatic groups with varying charges were synthesised: 1) PDADMAC quaternised with 1-chlorobutane (PD-C4); 2) 1-chloropentane (PD-C5); 3) 1-chlorodecane (PD-C10); 4) benzyl chloride (PDADMAC-BC); and 5) 4-fluoro benzylchloride (PDADMAC-BCF). PDADMAC was used as the standard to verify the performance of the synthesised polymers with prior studies [8, 14].

(Figure 1)

2.3.2 Free radical polymerisation of DMAEMA and its subsequent quaternisation

Following the same procedure as in the previous study [14], PDMAEMA and the best performing quaternised derivative from that study were synthesised. Briefly, the homopolymer was synthesised by simple bulk free radical polymerisation using AIBN as the initiator. Following the synthesis of the homopolymer, its quaternisation was carried out with 1-bromodecane at room temperature. PDMAEMA was used as the standard to verify the performance of the modified polymer and compare it with the prior study [14].

2.3.3 Jar testing

2.3.3.1 Synthetic DAF medium

To prepare the synthetic DAF influent water, cultured cells were diluted to 6×10^5 - 8×10^5 cells/mL with DI water buffered with 0.5 mM $NaHCO_3$ and brought to an ionic strength of 1.8 mM using NaCl. This was then adjusted to pH 7 using 1M HCl and 1M NaOH to maintain consistency and ensure comparability with previous studies [8, 14].

2.3.3.2 PosiDAF jar tests

A DAF Batch Tester, Model DBT6 (EC Engineering, Alberta, Canada), was used for the PosiDAF jar testing. The saturator influent and recycle flow consisted of DI water buffered with 0.5 mM $NaHCO_3$ and made up to an ionic strength of 1.8 mM with NaCl and corrected to pH 7. Industrial grade air was then used to pressurise the saturator to 450-470 kPa. The jar tests were conducted in batches of 1 L with synthetic DAF influent water. Flotation was conducted for 10 min prior to sampling of the treated effluent without any coagulation-flocculation. It should be noted that a recycle ratio of 20% was selected for all PosiDAF jar tests to ensure that a high bubble to particle ratio was maintained because conventional coagulation-flocculation of cells was not undertaken.

The polymer stock solutions were prepared and stirred at 200 rpm for 1 h before use. Aliquots of buffered solution were dosed with various polymer concentrations and added to the saturator prior to pressurisation. The performance of the polymers functionalised with hydrophobic moieties was compared against unmodified commercially available PDADMAC.

2.4 Characterisation and Analytical Methods

2.4.1 Cell characterisation

The cells were characterised by size using a Mastersizer 2000 (Malvern, Australia) and zeta potential using a Zetasizer Nano NZ (Malvern, Australia). These cell samples were analysed at the onset of the stationary phase during their growth cycles (10-13 days) and immediately prior to undertaking the jar tests.

2.4.2 ^{1}H NMR characterisation of polymers

The polymers were characterised using ^{1}H NMR spectra as recorded using a Bruker ACF300 (300 MHz) (Bruker, Germany) spectrometer. The de-methylated polymer was analysed by dissolving it in deuterated chloroform ($CDCl_3$) whereas the quaternised polyelectrolytes were analysed by employing deuterium oxide (D_2O) as solvent. The percent quaternisation was determined directly via the ratio of the signal areas from the experimental spectra of the modified polymer with that of PDADMAC and PDMAEMA.

2.4.3 Zeta potential and hydrodynamic size measurements

The synthesised polymers were characterised through zeta potential and hydrodynamic size measurements using a Zetasizer Nano ZS (Malvern, Australia), using 175° backscatter to measure Brownian motion *via* scattering intensity fluctuations. The dispersant parameters used for the analyses were RI: 1.330, Abs: 0.1 and diluent (water) viscosity: 0.88 cP. All samples were measured by scanning 15 times using automatic measurement settings. Assays were undertaken in triplicate.

2.4.4 Surface tension measurements of polymers in water

To quantify the hydrophobic nature of the polymers used in this study, the surface activity was measured by assessing the surface tension. A NIMA Surface Tensiometer equipped with a Du-

Nuoy ring was used to measure the surface tension of the polymer samples at room temperature. The solutions were first prepared at a concentration of 1 mg/mL in a buffer consisting of 1.8 mM NaCl and 0.5 mM $NaHCO_3$, adjusted to pH 7. Polymer stock solutions are typically known to take several hours to come to equilibrium which could result in large errors during physical measurements [32]. As a result these solutions were stirred at 200 rpm at room temperature for exactly 24 h before the measurements were made.

2.4.5 Charge density analysis

The charge densities of the polymers and algal cultures were assessed using a particle charge detector (PCD-04 Travel; Mütek BTG, Eclépens, Switzerland). The PCD-04 measures the charge density of a sample by titrating it with oppositely charged polyelectrolyte standard. To determine the charge polarity, streaming current detection is employed in which counter ions are segregated from their respective colloids *via* a reciprocating piston, resulting in a measurable current. Solutions of low molecular weight PDADMAC and sodium poly(ethylene sulphonate) (PES-Na) were used as titrants for anionic and cationic systems, respectively, at a concentration of 0.001 N. Charge density was calculated using the following equation:

$$\text{Charge Density} = \frac{C * V}{M} \qquad \text{(Equation 1)}$$

In which C is the titrant concentration (0.001 N), V is the volume of titrant used (L) and M is the mass of the sample in solution (g).

2.4.6 Bubble-polymer interaction characterisation using atomic force microscopy

Direct force measurements were carried out between two bubbles in solutions of PDADMAC-BCF, PDADMAC, PDMAEMA-C10 and PDMAEMA. From these measurements and the use of

the Chan-Dagastine-White (CDW) [33, 34] model, the surface potential of the microbubble interface could be ascertained. An Asylum MFP-3D atomic force microscope (Asylum Research, Santa Barbara) was used to conduct the measurements and cantilever spring constants were determined with the use of the Hutter and Bechhoefer method [35].

Prior to use, the glassware was soaked in a 10% Ajax detergent solution for 1 h and then a 10% nitric acid solution for 1 h. Milli-Q water (resistivity of 18 MΩ cm at 25 °C) was used to thoroughly rinse the glassware between each solution.

Custom cantilevers with the approximate dimensions of 480 μm × 50 μm × 2 μm and having a gold disc with a diameter of 45 μm located at the end were used [36]. The cantilevers were soaked in a solution of 1-decanethiol in ethanol [36, 37], making the gold disc hydrophobic, to allow a bubble to be attached to the gold disc. To ensure a suitable signal from the laser was received by the photodetector within the AFM, a layer of approximately 5 nm of chromium and then an approximate 10 nm layer of gold was sputter coated (Emitech K575X) onto the back of the cantilevers. The measured spring constants for the cantilevers used within these measurements were between 0.083 ± 0.01 N/m and 0.22 ± 0.02 N/m.

All measurements were conducted in the fluid cell designed for the AFM (Asylum Research) which has replaceable round glass surfaces. Before each measurement the hydrophobicity of the glass surfaces was increased by boiling them in *n*-propanol for 4 h [38]. Bubbles were generated ultrasonically (Undatim Ultrasonics D-reactor) onto the glass surfaces with a power of 25 W and a frequency of 515 kHz [39, 40]. This procedure was conducted within the desired solution and the generated bubbles had radii between 40 and 80 micrometres. Once bubbles were generated, the fluid cell was placed within the AFM and a prepared cantilever was lowered into solution.

With the use of an optical microscope (Nikon Ti-2000), the bubbles were sighted on the glass surface. The cantilever was lowered onto a suitable bubble and upon raising the cantilever the bubble was affixed to the gold disc of the cantilever. Another bubble on the surface was located and aligned axisymmetrically. This was achieved first with the optical microscope and subsequently with the piezo actuators of the AFM. Once the bubbles were aligned, direct force measurements were then performed. All collision velocities used within this work were below 300 nm/s to ensure that hydrodynamic fluid flow would not influence the forces of interaction between the colliding bubbles [41].

Upon completion of the direct force measurements, the CDW model was used to quantitatively describe the interaction forces between colliding bubbles. This model has been used and tested in previous studies [26, 27, 42] and accounts for interfacial deformation of bubbles during their collisions. This allows a model AFM force curve to be constructed based on fundamental surface force descriptions from theory, which is then compared to the experimentally gained force curve. The model requires the bubble radii, contact angles and interfacial tension to be experimentally measured as inputs into the calculation. This allows the surface potential, the only remaining free parameter within the calculation, of the bubble interface to be determined. In addition, at higher applied force between bubble or drop pairs, a simplified analytic formula derived from the CDW model has been developed that allows one to extract surface or interfacial tension from these types of force measurements between bubble or drop pairs. This method has routinely shown parity between the surface or interfacial tension values extracted from the AFM measurements and independently measured values via pendant drop at the same solution conditions [34].

2.4.7 Effluent analysis

Analysis of the treated water after the jar tests included measurement of algae cell concentration achieved by cell counting using a haemocytometer and Leica DM500 light microscope (Leica Microsystems Ltd, Switzerland) and measurement of the zeta potential of treated water using a Zetasizer Nano ZS (Malvern, Australia).

The residual polymer detection was carried out through fluorescence spectroscopy where fluorescence excitation emission matrices (F-EEMs) were obtained and analysed using a 1 cm path length quartz cuvette (Starna, Australia) and a Horiba Spectrophotometer. The F-EEMS were only obtained on effluent samples that were treated with PDADMAC-BC and PDADMAC-BCF due to the presence of benzene rings in the polymers that fluoresced at emission and excitation wavelengths of approximately 280 nm and 260 nm, respectively (Figure S6) [43, 44]. Fluorescence intensities were measured in triplicate at excitation wavelengths of 200–700 nm in 2 nm increments and emission wavelengths of 200–700 nm in 2 nm increments. The photomultiplier tube (PMT) voltage was set at 800 V and excitation and emission slit widths of 2 nm were utilised. Raman scans of MilliQ water in a sealed cell (Varian, Australia) were obtained at an excitation wavelength of 348 nm over the emission range of 380–410 nm, for the calculation of the area of the Raman peak. The area of the Raman peak was used to normalise the fluorescence intensity of all spectra, which were expressed in Raman units (RU). A linear calibration curve was obtained by making a plot of varying concentrations of PDADMAC-BC and PDADMAC-BCF against maximum intensity, as shown in SI Figures S4, S5.

3. RESULTS

3.1 Characterisation of algae and cyanobacteria

All the cells had similar spherical, unicellular morphology when grown in the laboratory and were comparable with previous studies [8, 21]. The physical diameter of the spherical cells of *C. vulgaris* CS-42/7 was 1.7 times larger than both the strains of *M. aeruginosa* (Table 1). Each of the three strains examined were found to have widely differing charge; for example, the CS-555/01 had a zeta potential of -17.0 ± 1.0 mV while that of the CS-564/01 and *C. vulgaris* CS-42/7 were -31.1 ± 1.0 mV and -27.6 ± 4.3 mV, respectively. Similarly, the charge density also varied with *C. vulgaris* having a charge that was almost 12 and 10 times lower (-0.96 ± 0.6 $x10^{-7}$ meq/cell) than that of *M. aeruginosa* CS-564/01 (-15.8 ± 0.8 $x10^{-7}$ meq/cell) and CS-555/1 (-9.3 ± 0.6 $x10^{-7}$ meq/cell), respectively. Although the cell diameters and charge characteristics for both *M. aeruginosa* cultures were similar to those described by Yap *et. al* [14], it was seen that the characteristics obtained for *C. vulgaris* were different from those described by Henderson *et. al* [15], illustrating the importance of undertaking such detailed characterisation studies.

(Table 1)

3.2 Characterisation of functionalised polymers

All polymers were cationic at pH 7 with the charge and zeta potentials varying from 1.21 to 6.55 meq/g and +30 mV to +65 mV, respectively (Table 2). It was observed that the charge densities of the hydrophobically modified PDADMAC polymers were less positive (4.1-4.3 meq/g) than that of commercially available PDADMAC (6.46 meq/g). In contrast, PDMAEMA functionalised with 1-bromodecane was found to have more than double the charge density (2.76 meq/g) in comparison to the unquaternised PDMAEMA (1.21 meq/g). Variations in the charge densities after modifications to the polymer backbone have been observed in previous studies

[21, 45] where factors such as alkylation and backbone protonation of the un-reacted repeat units were shown to influence the actual charge density of the polymers.

The modified polymers had higher surface tensions in comparison to their respective native scaffolds when measured using the Du-Nuoy ring method (Table 2). It was also seen that the surface tensions of all the PDADMAC polymers were greater than 65 mN/m when compared to the PDMAEMA polymers which were 44 - 69 mN/m in this study and in prior PosiDAF studies [14]. Additionally, PDADMAC polymers quaternised with aromatics displayed higher surface tensions (>71 mN/m) in comparison to the aliphatics which were in the range of 64-69 mN/m. The high surface tensions observed for PDADMAC polymers despite the inclusion of hydrophobic aromatic groups, are possibly due to the high concentrations of quaternary amine groups; the quaternisation completion was over 90% for PDADMAC polymers (Table 2) whereas in previous PDMAEMA studies it was 0-75% [21]. Similar observations were made in other studies where an increase in the surface tension was observed with an increased degree of quaternisation regardless of the side chain length [46, 47]. The high surface tension values demonstrate tendencies towards lower surface activity, indicating an overall affinity for the water phase and thus a shift in the hydrophile-lipophile balance (HLB). Therefore, characterising the surface activity of polymers on the microbubble surface rather than conventional determination of surface tension through Du-Nuoy ring method will provide a more appropriate characterisation of the hydrophobic nature of the polymers.

(Table 2)

3.3 Polymer-bubble interaction characterisation

With the exception of PDMAEMA-C10, the surface tensions of all polymers at the microbubble air-liquid interface were almost equivalent to that of Milli-Q water until the concentrations were increased to at least 0.5 mg/L (Table 3). The low surface tension (44 mN/m) observed for PDMAEMA-C10 at 0.3 mg/L indicates that this polymer adsorbed to the air-water interface more readily than the other polymers, possibly due to the migration of the hydrophobic alkyl groups to the air-water interface. Furthermore, an increase in the concentration of the same polymer resulted in a consequent increase in the surface activity (Table 3), which can be directly attributed to a greater surface density of polymer molecules at the interface.

While no coalescence was seen for bubbles coated with the PDMAEMA polymers, it was interesting to observe PDADMAC and PDADMAC-BCF coated bubbles coalescing at polymer concentrations of 2 mg/L (Table 3). However, it was also observed that when the concentration of PDADMAC-BCF was further increased to 5 mg/L, no coalescence was observed and the surface tension was seen to rapidly increase to 68 mN/m. The high surface tension of PDADMAC-BCF coated bubbles at 5 mg/L indicates little polymer adsorption on the bubble surface which was most likely due to an equilibrium existing between the polymer adsorbed at the gas-liquid interface and that free in bulk solution as hypothesised in a previous study [29].

Overall, the surface tension measurements from the AFM studies were found to contrast with those carried out by the Du-Nuoy ring method. For example, PDMAEMA-C10 had the highest surface tension as measured using a Du-Nuoy ring surface tensiometer and thus may have been expected to have the least attachment; however, in contrast, it was shown to readily adsorb on the bubble at a concentration of 0.3 mg/L. Furthermore, PDMAEMA which had the lowest surface tension (44 mN/m as detected by Du-Nuoy ring) was found to have poor polymer adsorption at 0.3 mg/L. These results show that conventional surface tension measurements of polymer

solutions by Du-Nuoy ring method do not elucidate polymer-bubble interactions when compared to measurements of surface activity of the polymers at the microbubble through advanced physical measurements such as AFM.

From Table 3, it is also seen that the bubble surface potentials as measured via AFM became more positive with increasing polymer dose and as the AFM surface tensions decreased. The surface potential ranged between -65 ± 15 mV at minimum, similar in magnitude to a that of bubble in the absence of surface active species [34], to +65 ± 15 mV at maximum polymer concentrations in line with the increasing adsorption of polymer onto the bubble surface with increasing polymer concentrations. However, large uncertainties in the surface potentials were observed for all the polymers and at all concentrations (Table 3). Similar uncertainties have been observed for surface potentials of bubbles coated with PDMAEMA and its variants [14], polyacrylamides [11] and non-polymers such as aluminium hydroxides [12] due to factors such as pH fluctuations [11] and polymer hydrolysis [11, 48, 49].

(Table 3)

3.4 Effect of hydrophobically functionalised polymers on cell removal for various algae

Results from jar tests demonstrated that maximum cell removals of *C. vulgaris* CS 42/7, *M. aeruginosa* CS-555/1 and *M. aeruginosa* CS-564/01 were 69% ± 3%, 38% ± 4%, 93% ± 4% , respectively (Figure 2, Appendix A Figures A1-A3). The effective separation of *M. aeruginosa* CS-564/01 is in line with previous observations made for *M. aeruginosa* CS-564/01 and CCAP-1450/3 [8, 9] where separation of 96% - 99% was observed. A similar decrease in separation effectiveness for a UK strain of *C. vulgaris* CCAP 211/11B [8] was also observed in comparison with *C .vulgaris* CS-42/7.

Micro-floc networks started to appear simultaneously as the cell removal of *C. vulgaris* CS-42/7 decreased at high doses of polymers. Interestingly, these micro-floc networks that formed during the 10 minute flotation period were clearly visible to the naked eye and possibly the result of coagulation-flocculation with the free polymer in water caused by turbulence in the system. Henderson *et al.*[8] suggested that at high doses, free polymers in the solution interact with the algal organic matter (AOM) thereby forming large suprastructures that cause steric repulsion with the high concentrations of polymer at the bubble surface, thereby impacting removal efficiency.

(Figure 2)

3.5 PosiDAF effluent

The initial zeta potential of the system with no added polymer was found to be −27.8 ± 4.5 mV for *C. vulgaris*, −12 ± 6.1 mV for *M. aeruginosa* CS-555/1, -31.1 ± 5.1 mV for *M. aeruginosa* CS-564/01 and, in each experiment, this did not change until at least 0.0005 meq/L of polymer had been added (Appendix A Figures A1-A3). From figure 3, it is seen that for all the cultures, a considerable change in the zeta potential, as well as a charge reversal took place. This was apparent for all polymers except PDADMAC-BCF and PDMAEMA-C10. Specifically, for PDADMAC-BCF and PDMAEMA-C10, the zeta potential seemed to remain stable between -22 to -11 mV and -19 to -6 mV, respectively. From Figure 3, it is also apparent that for the same polymers, the zeta potential at maximum cell removal was found to be lower than the other polymers trialled. This supports observations made by Yap *et al*. [14] who noted that polymers which have a strong hydrophobic character similar to surfactants have the best bubble adhesion as detected by stable zeta potentials and vice versa.

(Figure 3)

3.5.1 Residual polymer detection and quantification

When the treated effluent was tested for the presence of polymers (Figure 4), a polymer peak (P_1) was observed to fluoresce at 280 nm (emission) and 260 nm (excitation), tryptophan like (T_1) and chlorophyll a and b like (C_1 and C_2) peaks were emitted at 340 nm and 680 nm, respectively, and in line with results from prior studies [43, 44, 50]. It was also observed that the proportion of fluorinated polymer present in the treated effluent was nearly four to six times lower (~12% - 25%) than that of the non-fluorinate polymer which was found to have residual concentrations up to 85% of the initial polymer dose (Figure 5). The polymer residuals also slightly increased as the dose increased; this was particularly apparent for PDADMAC-BCF while treating *M. aeruginosa* CS-564/01 and *C. vulgaris* CS-42/7. This observation along with the decrease in cell removal at higher concentrations for *C. vulgaris* CS-42/7 (Appendix A Figure A2), suggests that steric interactions between the polymer-AOM aggregates with polymer on the bubbles contribute to the fluctuations in cell removal observed in PosiDAF as hypothesised previously [8]. The results obtained while evaluating PDADMAC-BCF concentrations in the treated water also corroborate well with the charge measurements observed in Figure 3 wherein the fluorinated polymer was found to have highly stable negative zeta potential. This observation therefore, clearly indicates a lower concentration of the polymer in the treated effluent and lower chemical contamination ahead of further pre-treatment.

(Figure 4) (Figure 5)

4. DISCUSSION

It was previously hypothesised that the incorporation of hydrophobic groups on the polymer backbone might lead to enhanced attachment of cationic HMPs to microbubble surfaces relative to those without any modification, and thus reduced polymer in the effluent. In this study, highly stable anionic zeta potentials of treated water were observed, indicating a low effluent polymer concentration, but only with two HMPs, namely PDMAEMA-C10 and PDADMAC-BCF (Figure 3). The presence of alkyl side chains in PDMAEMA-C10 has been shown to facilitate a stronger association to the bubble surface by providing sites for hydrophobic interactions [14]. This phenomenon forces the polymers to adopt a 'flat and tight' conformation on the bubble due to their interactions with the cells and the AOM were impacted (Figure 6). On the contrary, the aryl side chains of PDADMAC-BC and PDADMAC-BCF are known to stack on top of each other due to π-π interactions as seen in graphene oxide based flocculants [51-55]. This stacking is speculated to force the polymer chains to project away from the bubble and prevent hydrophobic association of the HMP with the bubble, thereby causing poor polymer-bubble adhesion. This was evidenced in the case of PDADMAC-BC treated effluent where over 70% of the initial polymer dose and a highly positive zeta potential was detected. However, for PDADMAC-BCF, the effluent analyses suggest another mechanism is at play to counter-balance the stacking effect. It is likely that this is due to the presence of fluorine molecules within the polymer, which are known to re-orient itself at the air-water interface and adsorb ahead of the three phase contact line on hydrophobic interfaces [56, 57]. While the π-π stacking due to the aryl groups causes the chains to project away from the bubble, the presence of fluorine molecules help the chains to anchor on the bubble surface, resulting in a balance between polymer association to the interface and chain projection away from the bubble (Figure 6). This configuration would imply that more steric interactions would be encountered and consequently less polymer and charge would

occupy the same area on a microbubble surface resulting in low surface potential [8, 58]. The AFM data from Table 3 shows that this phenomenon is particularly evident for PDADMAC-BCF wherein the surface tensions increased to 68 mN/m after an initial decrease to 58 mN/m. However, it is to be noted that the counter balancing effect of the fluorine in PDADMAC-BCF was not apparent at lower concentrations as poor polymer-bubble adhesion was seen at 0.3 mg/L (Table 3). Therefore, this indicates that the concentrations of polymers dosed have a direct impact on the polymer configuration on the bubble surface and could be critical to the outcome of the PosiDAF process.

Apart from the polymer configurations, the concentrations of the polymers dosed were also seen to have a profound impact on polymer adsorption on the bubble. For example, the rapid decrease in cell removal from 70% to 35% for *C. vulgaris* CS-42/7 along with the zeta potential of the treated effluent at higher concentrations of the HMPs, indicates inconsistencies in polymer adsorption onto the bubbles (Appendix A Figure A2). This is supported by the fact that at concentrations of 2 mg/L or higher, the adsorption of PDADMAC polymers on bubbles was vacillating (Table 3). In a previous study, the adsorption of various surfactants such as dodecyl-, cetyl-, and octadecyltrimethylammonium bromide on the microbubble surface were hypothesised to be impacted due to equilibrium shifts between surfactants adsorbed at the gas-liquid interface and those free in bulk solution [29]. Similarly, it is suggested that equilibrium shifts between polymers adsorbed at the gas-liquid interface and those free in bulk solution to drive polymer adsorption to and from bubbles (Figure 6). Consequently, such shifts during DAF experiments as a result of rapid change in concentrations from t = 0 min to t = 10 mins are theorised to cause variations in polymer orientation on the bubble surface thereby eventually impacting cell removal.

(Figure 6)

5. CONCLUSION

The specific conclusions drawn from this work are as follows:

- Hydrophobic modification of PDADMAC with various pendant groups for bubble surface modification in PosiDAF was successful and the results indicate that all the polymers trialled achieved increased or comparable cell removal when compared to prior studies that utilised commercially available PDADMAC and hydrophobically modified PDMAEMA.
- Stable negative zeta potentials between -22 mV and -6 mV were observed in PosiDAF treated effluent across the entire dose range and for all species when PDADMAC-BCF and PDMAEMA-C10 were used as the bubble modification chemicals. Furthermore, the zeta potential of these two polymer treated effluents at maximum cell removal was found to be lower than the other polymers trialled. This indicates that very low amounts of the polymer remained in the treated water, thereby confirming better adhesion of the polymer to the bubble surface.
- Aromatically substituted polymers (PDADMAC-BC and PDADMAC-BCF) were quantifiable for residual polymers in the treated effluent through F-EEM analysis. It was observed that the treated effluent concentration of PDADMAC-BCF was four to six times less than that when using PDADMAC-BC.
- The adsorption conformation of the polymer on the bubble surface alters dependent on both the polymer backbone and the type of hydrophobic moiety incorporated. PDMAEMA and its derivative were found to adsorb very tightly to the bubble surface

unlike PDADMAC derivatives which tend to project away from the into the surrounding matrix as evidenced by the AFM results.

ACKNOWLEDGEMENTS

This research was partially supported under Australian Research Council's Linkage Projects funding scheme (project number LP0990189) and an Australian Commonwealth Research Training Program (RTP) Scholarship received by Mr Narasinga Rao Hanumanth Rao. This work was also performed in part at the Melbourne Centre for Nanofabrication (MCN) in the Victorian Node of the Australian National Fabrication Facility (ANFF) and in the Materials Characterisation and Fabrication Platform (MCFP) at the University of Melbourne. The authors would like to thank the UNESCO Centre for Membrane Science and Technology (University of New South Wales) and Particle Fluids Processing Centre (University of Melbourne) for providing infrastructure support over the duration of this work.

REFERENCES

1. Burns, S.E., S. Yiacoumi, and C. Tsouris, *Microbubble generation for environmental and industrial separations.* Separation and Purification Technology, 1997. **11**(3): p. 221-232.
2. Karhu, M., T. Leiviskä, and J. Tanskanen, *Enhanced DAF in breaking up oil-in-water emulsions.* Separation and Purification Technology, 2014. **122**(0): p. 231-241.
3. Garg, S., L. Wang, and P.M. Schenk, *Flotation separation of marine microalgae from aqueous medium.* Separation and Purification Technology, 2015. **156**: p. 636-641.
4. Englert, A.H., R.T. Rodrigues, and J. Rubio, *Dissolved air flotation (DAF) of fine quartz particles using an amine as collector.* International Journal of Mineral Processing, 2009. **90**(1–4): p. 27-34.
5. Fang, R., X. Cheng, and X. Xu, *Synthesis of lignin-base cationic flocculant and its application in removing anionic azo-dyes from simulated wastewater.* Bioresource Technology, 2010. **101**(19): p. 7323-7329.
6. Gehr, R. and J.G. Henry, *The adsorption behaviour of cationic polyelectrolytes in dissolved air flotation.* Water Pollut Res and Control, Proc of the Bienn Conf of the Int Assoc On Water Pollut Res and Control, 11th, 1982. **14**(6-7 /7): p. 689-704.
7. Ahmad, A.L., et al., *Optimization of microalgae coagulation process using chitosan.* Chemical Engineering Journal, 2011. **173**(3): p. 879-882.
8. Henderson, R.K., S.A. Parsons, and B. Jefferson, *Polymers as bubble surface modifiers in the flotation of algae.* Environmental Technology, 2010. **31**(7): p. 781-790.

9. Malley Jr, J.P., *The use of selective and direct DAF for removal of particulate contaminants in drinking water treatment.* Water Science and Technology, 1995. **31**(3–4): p. 49-57.
10. Oliveira, C., R.T. Rodrigues, and J. Rubio, *Nucleation, growth and coalescence phenomena of air bubbles on quartz particles in different aqueous solutions.* Bubble Science, Engineering and Technology, 2014. **5**(1-2): p. 15-24.
11. Oliveira, C. and J. Rubio, *Zeta potential of single and polymer-coated microbubbles using an adapted microelectrophoresis technique.* International Journal of Mineral Processing, 2011. **98**(1–2): p. 118-123.
12. Han, M.Y., M.K. Kim, and M.S. Shin, *Generation of a positively charged bubble and its possible mechanism of formation.* Journal of Water Supply: Research and Technology - AQUA, 2006. **55**(7-8): p. 471-478.
13. Henderson, R.K., S.A. Parsons, and B. Jefferson, *The potential for using bubble modification chemicals in dissolved air flotation for algae removal.* Separation Science and Technology, 2009. **44**(9): p. 1923-1940.
14. Yap, R.K.L., et al., *Hydrophobically-associating cationic polymers as micro-bubble surface modifiers in dissolved air flotation for cyanobacteria cell separation.* Water Research, 2014. **61**: p. 253-262.
15. Henderson, R., S.A. Parsons, and B. Jefferson, *The impact of algal properties and pre-oxidation on solid–liquid separation of algae.* Water Research, 2008. **42**(8–9): p. 1827-1845.
16. Henderson, R.K., S.A. Parsons, and B. Jefferson, *The impact of differing cell and algogenic organic matter (AOM) characteristics on the coagulation and flotation of algae.* Water Research, 2010. **44**(12): p. 3617-3624.
17. Pivokonsky, M., et al., *The impact of algogenic organic matter on water treatment plant operation and water quality: A review.* Critical Reviews in Environmental Science and Technology, 2016. **46**(4): p. 291-335.
18. Teixeira, M.R. and M.J. Rosa, *Comparing dissolved air flotation and conventional sedimentation to remove cyanobacterial cells of Microcystis aeruginosa.* Separation and Purification Technology, 2006. **52**(1): p. 84-94.
19. Teixeira, M.R. and M.J. Rosa, *Comparing dissolved air flotation and conventional sedimentation to remove cyanobacterial cells of Microcystis aeruginosa.* Separation and Purification Technology, 2007. **53**(1): p. 126-134.
20. Henderson, R., et al., *PosiDAF™: Simplifying Algal Cell Separation Through Process Intensification.* Asia Pacific Confederation of Chemical Engineering Congress 2015: APCChE 2015, incorporating CHEMECA 2015, 2015.
21. Yap, R., *Polymer coated bubbles in dissolved air flotation for processing algae laden water*, in *School of Civil and Environmenal Engineering*. 2013, University of New South Wales: Sydney.
22. Ríos, H.E., et al., *Surface properties of cationic polyelectrolytes hydrophobically modified.* Colloids and Surfaces A: Physicochemical and Engineering Aspects, 2011. **384**: p. 262-267.
23. Vuillaume, P.Y., et al., *Ordered Polyelectrolyte "Multilayers". 6. Effect of Molecular Parameters on the Formation of Hybrid Multilayers Based on Poly(Diallylammonium) Salts and Exfoliated Clay.* Chemistry of Materials, 2003. **15**(19): p. 3625-3631.
24. Haarhoff, J. and J.K. Edzwald, *Dissolved air flotation modelling: Insights and shortcomings.* Journal of Water Supply: Research and Technology - AQUA, 2004. **53**(3): p. 127-150.
25. Milling, A.J., *Depletion and structuring of sodium poly(styrenesulfonate) at the silica-water interface.* Journal of Physical Chemistry, 1996. **100**(21): p. 8986-8993.
26. Browne, C., et al., *Direct AFM force measurements between air bubbles in aqueous polydisperse sodium poly(styrene sulfonate) solutions: Effect of collision speed, polyelectrolyte concentration and molar mass.* Journal of Colloid and Interface Science, 2015. **449**: p. 236-245.

27. Browne, C., et al., *Direct AFM force measurements between air bubbles in aqueous monodisperse sodium poly(styrene sulfonate) solutions.* Journal of Colloid and Interface Science, 2015. **451**: p. 69-77.
28. Becker, N.S.C., et al., *Detection of polyelectrolytes at trace levels in water by fluorescent tagging.* Reactive and Functional Polymers, 2004. **60**(0): p. 183-193.
29. Henderson, R.K., S.A. Parsons, and B. Jefferson, *Surfactants as bubble surface modifiers in the flotation of algae: Dissolved air flotation that utilizes a chemically modified bubble surface.* Environmental Science and Technology, 2008. **42**(13): p. 4883-4888.
30. Bolch, C.S. and S. Blackburn, *Isolation and purification of Australian isolates of the toxic cyanobacteriumMicrocystis aeruginosa Kütz.* Journal of Applied Phycology, 1996. **8**(1): p. 5-13.
31. Bazito, R.C., F.L. Cássio, and F.H. Quina, *Synthesis and characterization of chiral [3,22]-ionenes.* Macromolecular Symposia, 2005. **229**: p. 197-202.
32. Riess, G., *Micellization of block copolymers.* Progress in Polymer Science, 2003. **28**(7): p. 1107-1170.
33. Chan, D.Y.C., R.R. Dagastine, and L.R. White, *Forces between a Rigid Probe Particle and a Liquid Interface. I. The Repulsive Case.* Journal of Colloid and Interface Science, 2001. **236**(1): p. 141-154.
34. Tabor, R.F., et al., *Measurement and analysis of forces in bubble and droplet systems using AFM.* Journal of Colloid and Interface Science, 2012. **371**(1): p. 1-14.
35. Hutter, J.L. and J. Bechhoefer, *Calibration of atomic-force microscope tips.* Review of Scientific Instruments, 1993. **64**(7): p. 1868-1873.
36. Vakarelski, I.U., et al., *Dynamic interactions between microbubbles in water.* Proceedings of the National Academy of Sciences of the United States of America, 2010. **107**(25): p. 11177-11182.
37. Mir, Y., P. Auroy, and L. Auvray, *Density profile of polyelectrolyte brushes.* Physical Review Letters, 1995. **75**(15): p. 2863-2866.
38. Biggs, S. and F. Grieser, *Atomic force microscopy imaging of thin films formed by hydrophobing reagents.* Journal of Colloid and Interface Science, 1994. **165**(2): p. 425-430.
39. Balasuriya, T.S. and R.R. Dagastine, *Interaction forces between bubbles in the presence of novel responsive peptide surfactants.* Langmuir, 2012. **28**(50): p. 17230-17237.
40. Vakarelski, I.U., et al., *Bubble colloidal AFM probes formed from ultrasonically generated bubbles.* Langmuir, 2008. **24**(3): p. 603-605.
41. Manor, O., et al., *Dynamic Forces between Bubbles and Surfaces and Hydrodynamic Boundary Conditions.* Langmuir, 2008. **24**(20): p. 11533-11543.
42. Tabor, R.F., et al., *Anomalous Stability of Carbon Dioxide in pH-Controlled Bubble Coalescence.* Angewandte Chemie, 2011. **123**(15): p. 3516-3518.
43. Schwarz, F.P. and S.P. Wasik, *Fluorescence measurements of benzene, naphthalene, anthracene, pyrene, fluoranthene, and benzo(e)pyrene in water.* Anal Chem, 1976. **48**(3): p. 524-8.
44. Birks, J.B., C.L. Braga, and M.D. Lumb, *'Excimer' Fluorescence. VI. Benzene, Toluene, p-Xylene and Mesitylene.* Proceedings of the Royal Society of London. Series A. Mathematical and Physical Sciences, 1965. **283**(1392): p. 83-99.
45. Kim, C.-R. and H.-S. Byun, *Effect of cosolvent on the phase behavior of binary and ternary mixture for the poly(2-dimethylaminoethyl methacrylate) in supercritical solvents.* Fluid Phase Equilibria, 2014. **381**(0): p. 51-59.
46. Ni, P., et al., *Poly (dimethylamino) ethyl methacrylate for use as a surfactant in the miniemulsion polymerization of styrene.* Langmuir, 2006. **22**(14): p. 6016-6023.
47. Vamvakaki, M., et al., *Effect of partial quaternization on the aqueous solution properties of tertiary amine-based polymeric surfactants: Unexpected separation of surface activity and cloud point behavior.* Macromolecules, 2001. **34**(20): p. 6839-6841.

48. Holmberg, K., et al., *Surfactants and polymers in aqueous solution*. 2003: Wiley.
49. Bolto, B. and J. Gregory, *Organic polyelectrolytes in water treatment.* Water Research, 2007. **41**(11): p. 2301-2324.
50. Henderson, R., et al., *Fluorescence as a potential monitoring tool for recycled water systems: a review.* Water research, 2009. **43**(4): p. 863-881.
51. Hyung, H., et al., *Natural organic matter stabilizes carbon nanotubes in the aqueous phase.* Environmental Science & Technology, 2007. **41**(1): p. 179-184.
52. Chen, D., H. Feng, and J. Li, *Graphene Oxide: Preparation, Functionalization, and Electrochemical Applications.* Chemical Reviews, 2012. **112**(11): p. 6027-6053.
53. Hartono, T., et al., *Layer structured graphite oxide as a novel adsorbent for humic acid removal from aqueous solution.* Journal of Colloid and Interface Science, 2009. **333**(1): p. 114-119.
54. Yang, X., et al., *Graphene oxide-iron oxide and reduced graphene oxide-iron oxide hybrid materials for the removal of organic and inorganic pollutants.* RSC Advances, 2012. **2**(23): p. 8821-8826.
55. Zhao, G., et al., *Sulfonated Graphene for Persistent Aromatic Pollutant Management.* Advanced Materials, 2011. **23**(34): p. 3959-3963.
56. Mukerjee, P. and T. Handa, *Adsorption of fluorocarbon and hydrocarbon surfactants to air-water, hexane-water and perfluorohexane-water interfaces. Relative affinities and fluorocarbon-hydrocarbon nonideality effects.* The Journal of Physical Chemistry, 1981. **85**(15): p. 2298-2303.
57. Kovalchuk, N.M., et al., *Fluoro- vs hydrocarbon surfactants: Why do they differ in wetting performance?* Advances in Colloid and Interface Science, 2014. **210**(0): p. 65-71.
58. Napper, D.H., *Polymeric Stabilization of Colloidal Dispersions.* Academic Press, London., 1983.

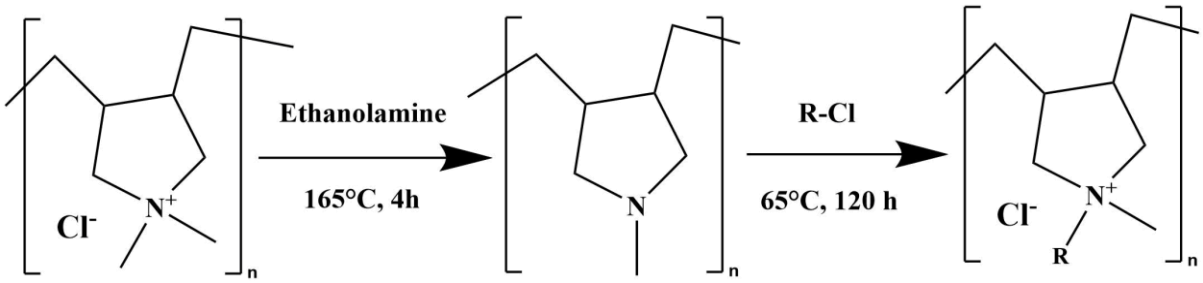

Figure 1. Reaction scheme indicating de-methylation and quaternisation of the de-methylated PDADMAC.

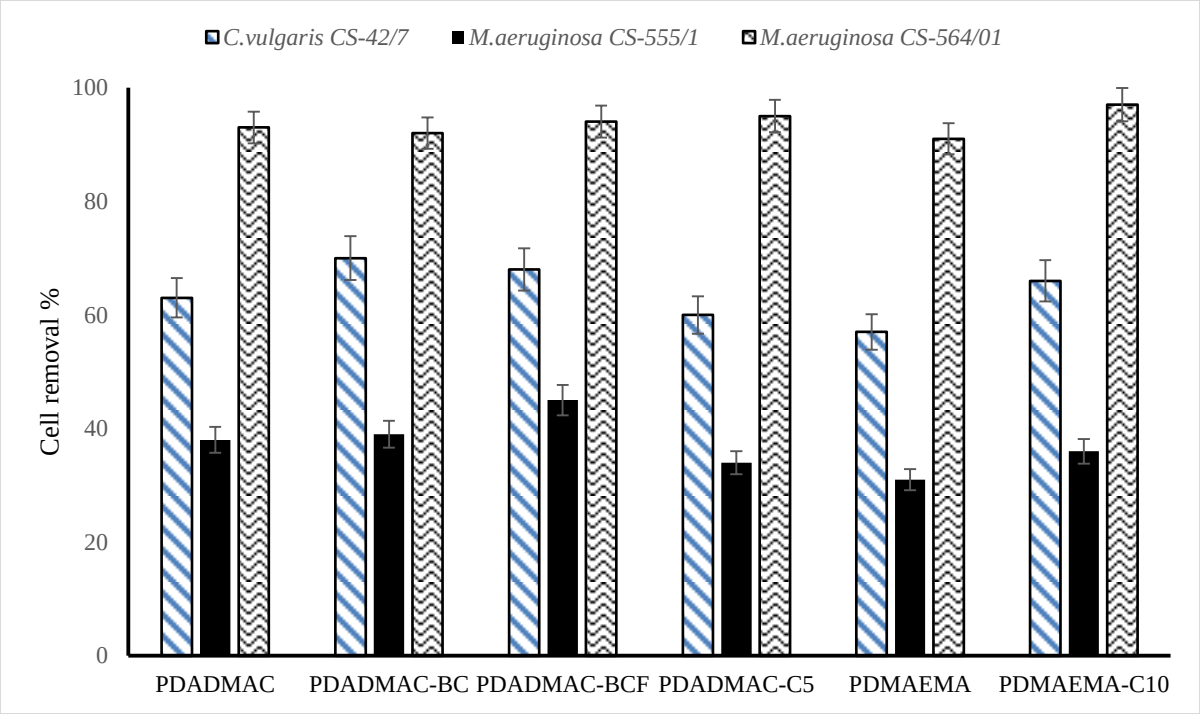

Figure 2. Maximum removal efficiencies for PDADMAC, PDADMAC-BC, PDADMAC-BCF, PDADMAC-C5, PDMAEMA and PDMAEMA-C10 when treating *C. vulgaris* – CS 42/7, *M. aeruginosa*- CS 555/1, *M. aeruginosa*- CS 564/01. For full dataset, refer to Figures A1-A3 in Appendix A.

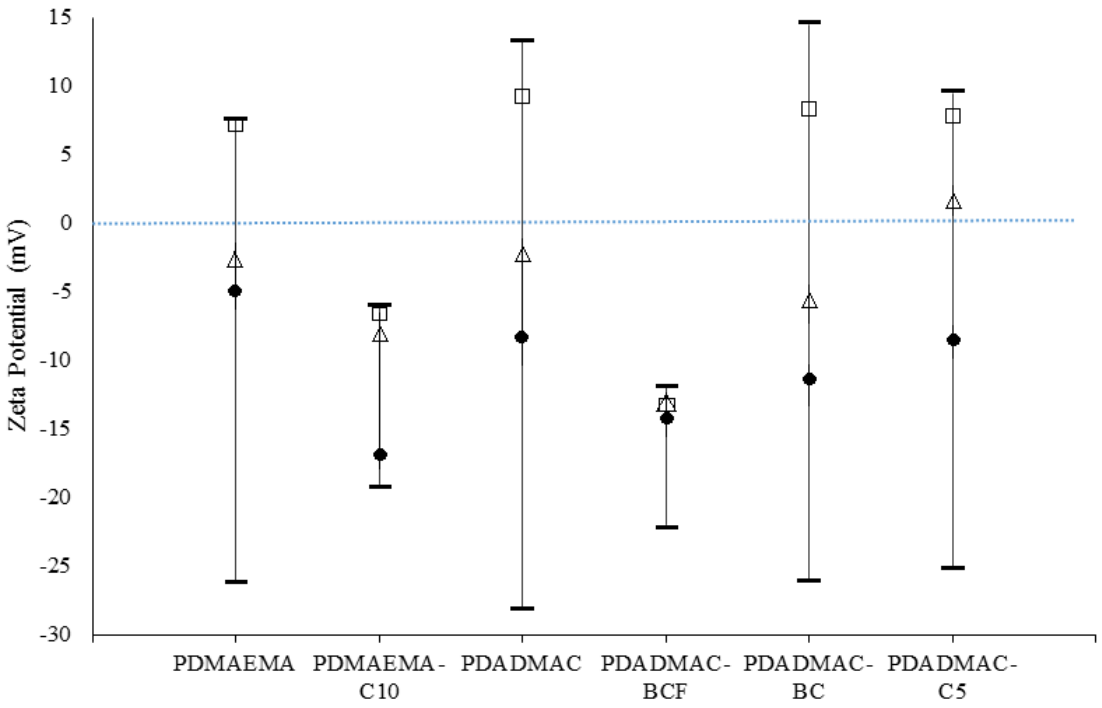

Figure 3. Comparison of the zeta potential ranges obtained for the treated effluent for the full dose ranges of PDMAEMA, PDMAEMA-C10, PDADMAC, PDADMAC-BCF, PDADMAC-BC, PDADMAC-C5 on *C. vulgaris* CS-42/7, *M. aeruginosa* CS-555/1 and *M. aeruginosa* CS-564/01. (●), (□), (△) represent zeta potential at maximum removal of *C. vulgaris*, *M. aeruginosa* CS-555/1 and CS-564/01, respectively. For full dataset, refer to Figures A1-A3 in Appendix A.

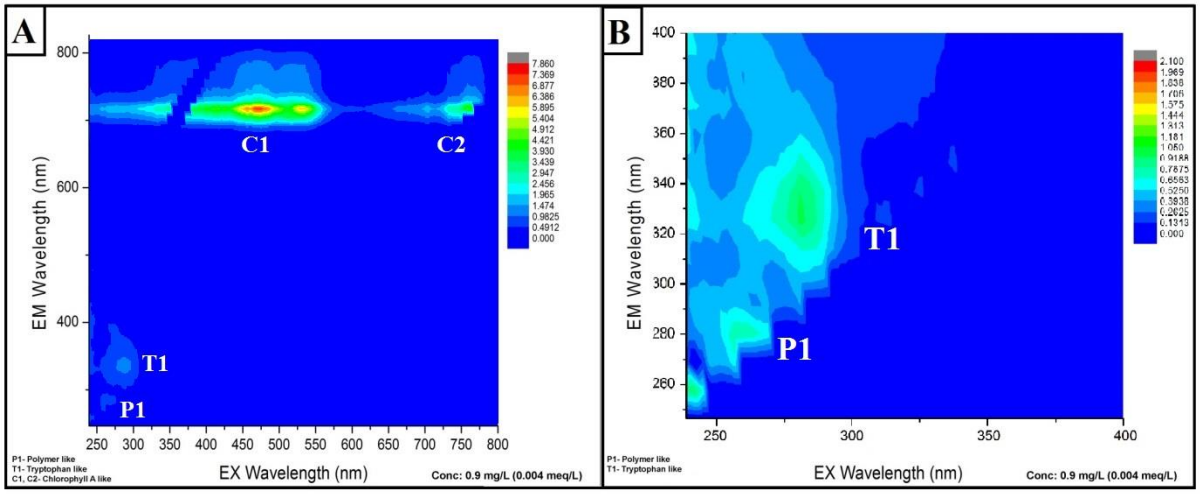

Figure 4. (A) Fluorescence excitation emission matrix (F-EEM) obtained while testing PDADMAC-BCF treated effluent of *C. vulgaris* CS-42/7. P1 indicates the polymer like regions while T1, C1 and C2 indicate the tryptophan-like, chlorophyll a and *b* regions, respectively. Initial PDADMAC-BCF concentration – 0.9 mg/L (0.004 meq/L). (B) F-EEM magnified to isolate regions within 240-400 nm excitation and 240-400 nm emission.

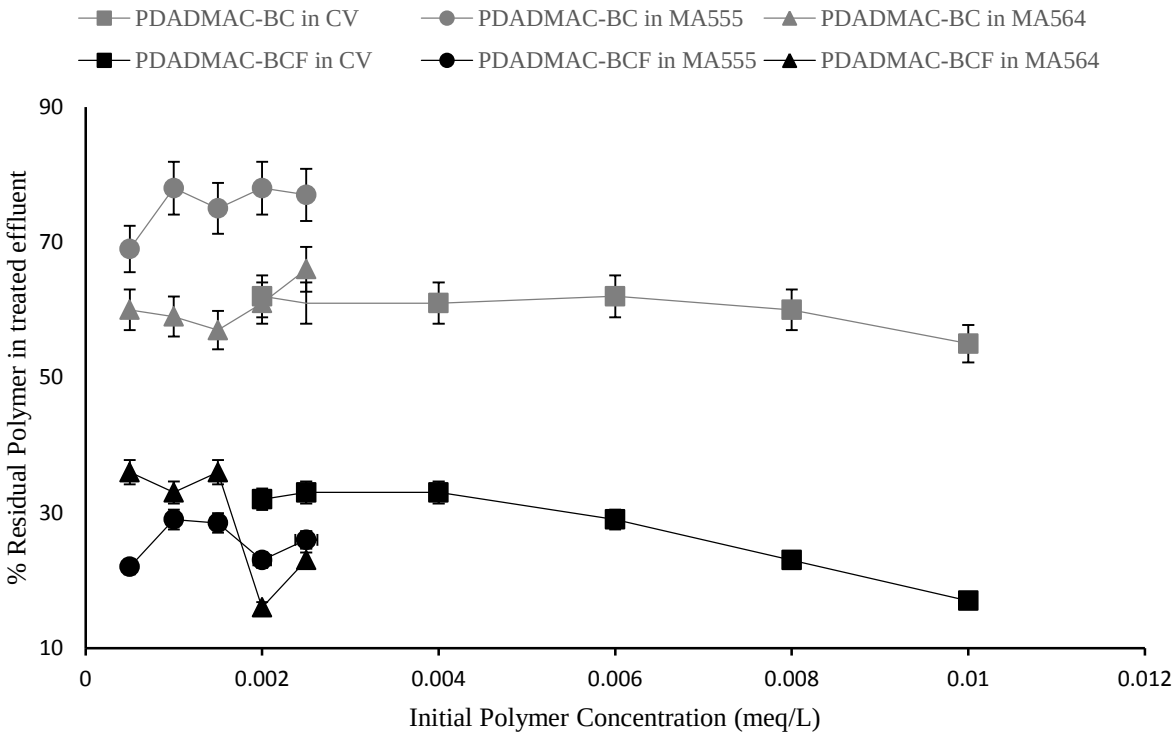

Figure 5. Proportion of the initial polymer concentration dosed in PosiDAF experiments remaining in treated effluent on treating CV (*C. vulgaris* CS-42/7), MA555 (*M. aeruginosa* CS-555/1) and MA564 (*M. aeruginosa* CS-564/01). The polymers tested were PDADMAC-BC and PDADMAC-BCF.

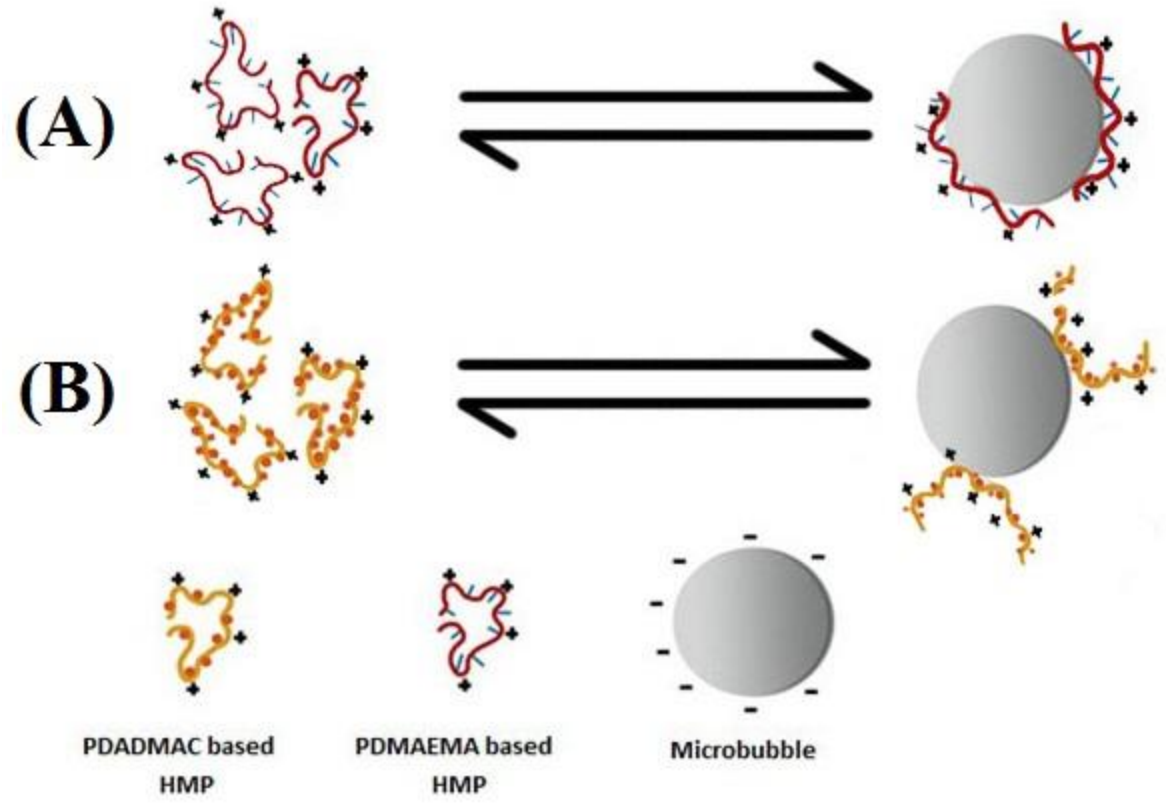

Figure 6. Schematic depicting the equilibrium between polymer adsorbed on the bubble and that free in bulk solution and the impact of alkyl and aryl side chains on hydrophobic association with the bubble; (A) - Flat and tight configuration of PDMAEMA polymers on the bubble (B) – Loosely bound configuration of PDADMAC polymers on the bubble.

Table 1. Physicochemical characteristics of *M. aeruginosa* (CS-5555/01, CS-564/01 and CCAP-1450/3) and *C. vulgaris* (CS-42/7 and CCAP 211/11B)

Properties	**Diameter**	**Average cell concentration at the onset of stationary phase**	**Zeta Potential**	**Charge Density**
Units	µm	$\times 10^{7}$ cells mL^{-1}	mV	$\times 10^{-7}$ meq $cell^{-1}$
CS-555/01	3.0 ± 0.7	1.79 ± 0.08	-17.0 ± 1.0	-9.3 ± 0.6
CS-564/01	3.1 ± 0.6	2.01 ± 0.12	-32.8 ± 0.6	-15.8 ± 0.8
CS-42/7	5.2 ± 0.6	1 ± 0.3	-27.6 † 4.3	-0.96 ± 0.6
CCAP-1450/3 †‡	5.4 ± 0.8 †	-	-19.8 ± 1.5 †	-0.02 ‡
CCAP – 211/11B †‡	4 ± 1.1 †	-	-32.3 ± 0.6 †	-0.85 ‡

'-' indicates no data available

† Data obtained or calculated from Henderson *et al.* (2010) [22]

‡ Data obtained or calculated from Henderson *et al.* (2010) [30]

Table 2. Characterisation of polyelectrolytes used in PosiDAF jar tests

Polymer	PDADMAC	PDADMAC–C5	PDADMAC–C10	PDADMAC–BC	PDADMAC–BCF	PDMAEMA	PDMAEMA-C10
Structure	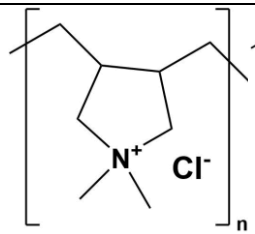	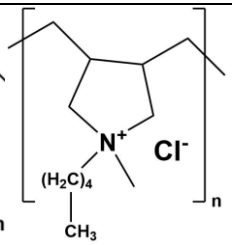	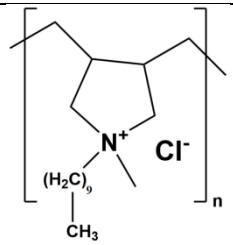	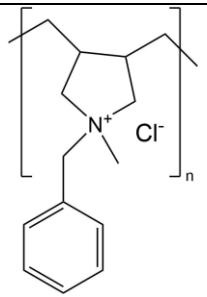	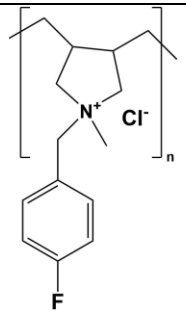	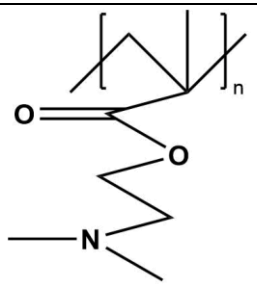	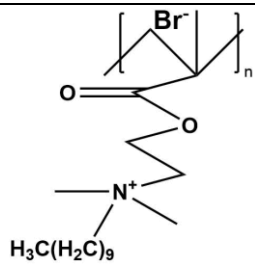
Quaternisation Completion (%)	100	92.2	Not measured as polymer did not go into solution	93.8	90.9	N/A	52
Charge Density (meq/g)	6.46 ± 0.2	4.33 ± 0.21		4.1 ± 0.2	4.17 ± 0.08	1.21	2.76
Zeta Potential (mV)	55.6 ± 7.06	37.8 ± 8.2		52.4 ± 2.69	55.3 ± 6.3	49.1 ± 3.5	59.8 ± 1.2
Surface Tension (mN/m)	69 ± 1	64.1 ± 0.5		73.5 ± 0.1	71.9 ± 0.5	44 ± 0.3	69 ± 0.1

Table 3. Characterisation of polymer coated bubbles in PosiDAF at pH 7

Polymer used to modify bubble	Concentration (mg/L)	Surface Potential (mV)	Surface Tension calculated from AFM force curve (mN/m)
PDMAEMA	0.3	-65 ± 15	70
	0.5	+55 ± 25	58
	2.0	+50 ± 30	51
PDMAEMA-C10	0.3	+65 ± 15	44
	0.5	+60 ± 20	42
	2.0	+65 ± 15	40
PDADMAC-BCF	0.3	-65 ± 15	71
	0.5	+55 ± 25	58
	2.0	Coalesce – bridging	N/A
	5.0	+45 ± 5	68
PDADMAC	0.3	-65 ± 15	71
	0.5	-65 ± 15	71
	2.0	Coalesce – bridging	44, then 31

Appendix A

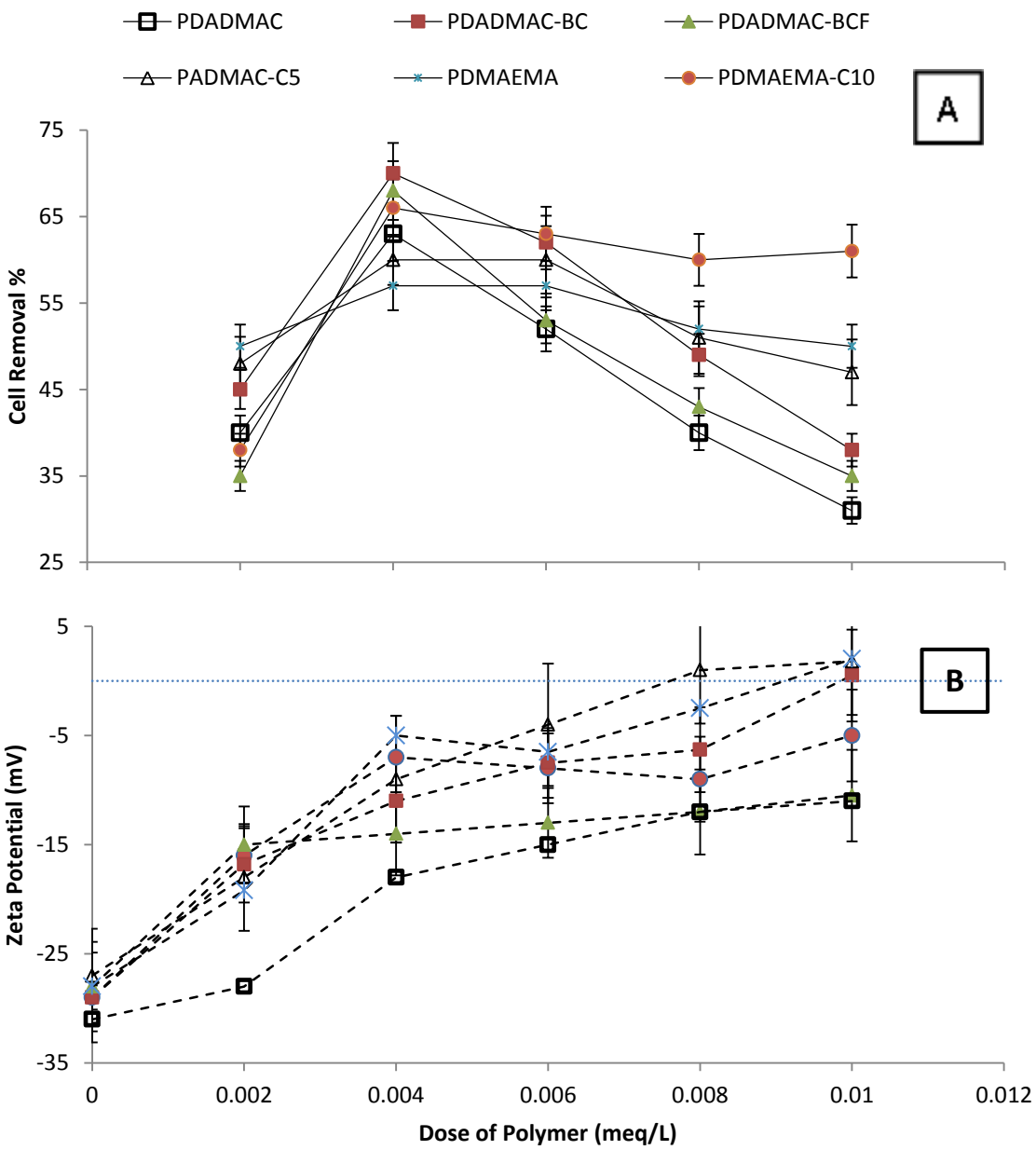

Figure A1. Comparison of PosiDAF performance with PDADMAC, PDADMAC-C5, PDADMAC -BC, PDADMAC -BCF, PDMAEMA and PDMAEMA-C10 on *C. vulgaris* CS-

42/7; A – Cell removal efficiency and B – Zeta Potential of effluent Vs Dose of PDADMAC, PDADMAC-C5, PDADMAC-BC, PDADMAC-BCF, PDMAEMA and PDMAEMA-C10;

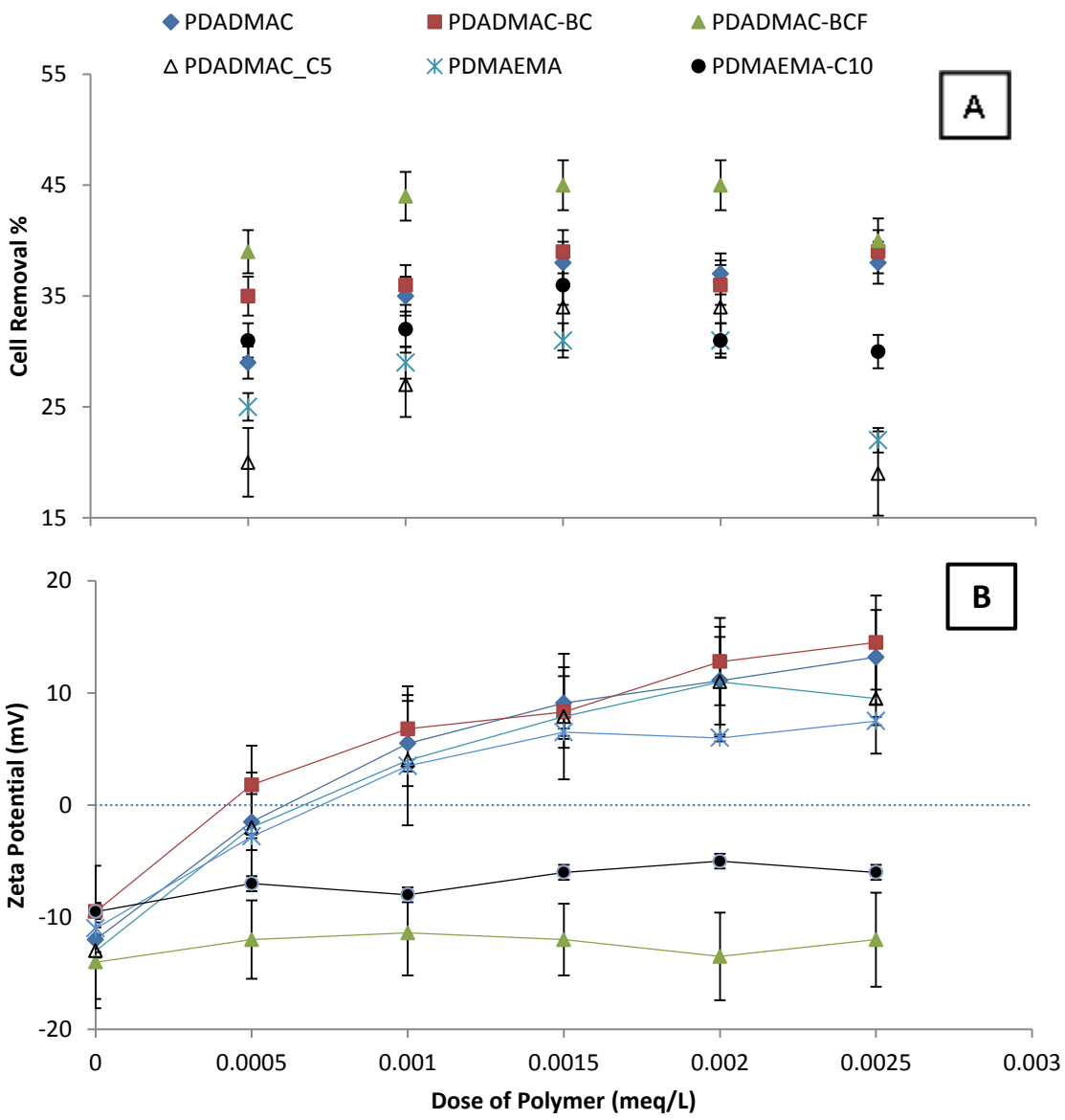

Figure A2. Comparison of PosiDAF performance with PDADMAC, PDADMAC-C5, PDADMAC-BC, PDADMAC-BCF, PDMAEMA and PDMAEMA-C10 on *M. aeruginosa* CS-555/1; A – Cell removal efficiency and B – Zeta Potential of effluent Vs Dose of PDADMAC, PDADMAC-C5, PDADMAC-BC, PDADMAC-BCF, PDMAEMA and PDMAEMA-C10;

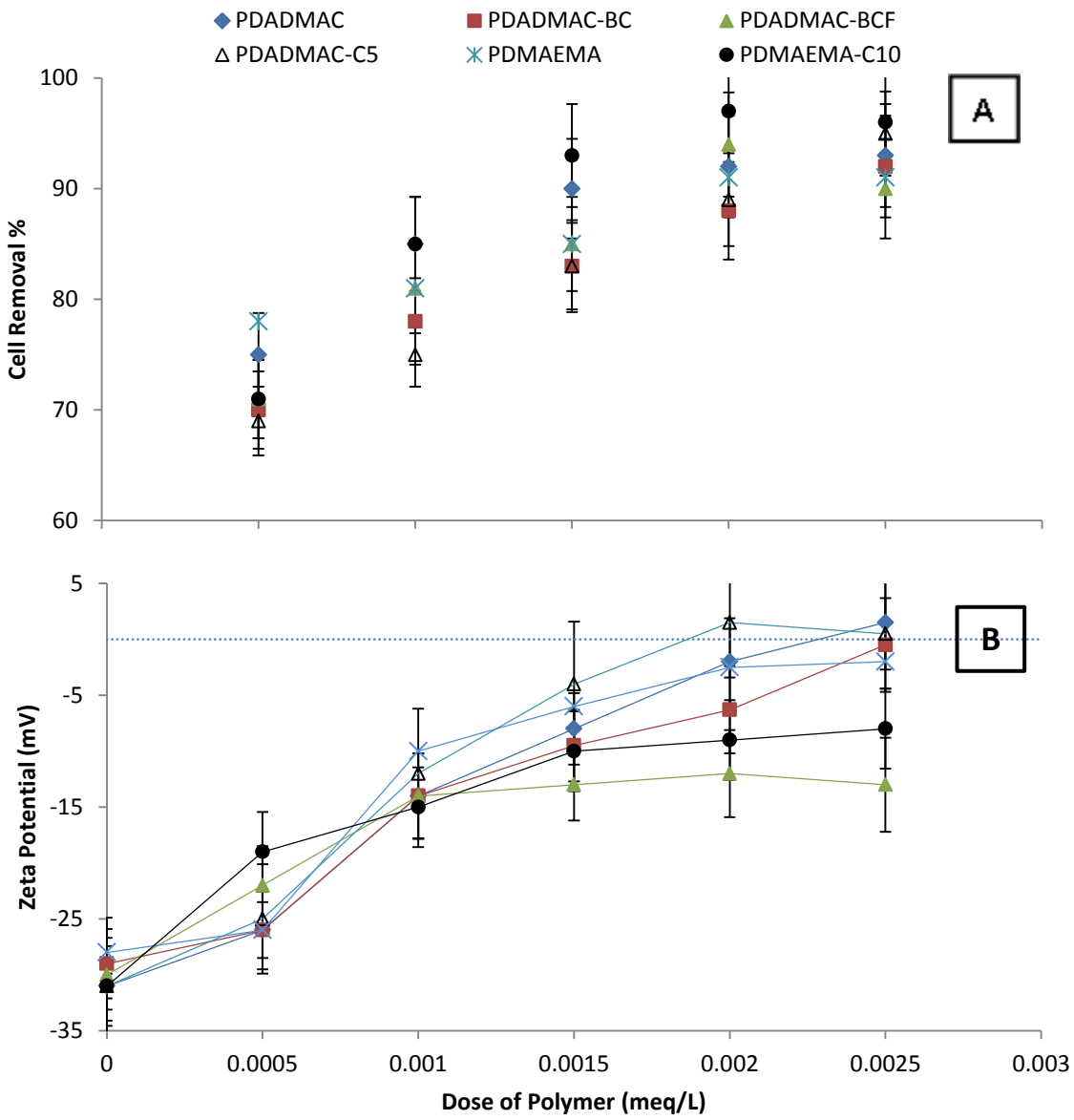

Figure A3. Comparison of PosiDAF performance with PDADMAC, PDADMAC-C5, PDADMAC-BC, PDADMAC-BCF, PDMAEMA and PDMAEMA-C10 on *M. aeruginosa* CS-564/01; A – Cell removal efficiency and B – Zeta Potential of effluent Vs Dose of PDADMAC, PDADMAC-C5, PDADMAC-BC, PDADMAC-BCF, PDMAEMA and PDMAEMA-C10;

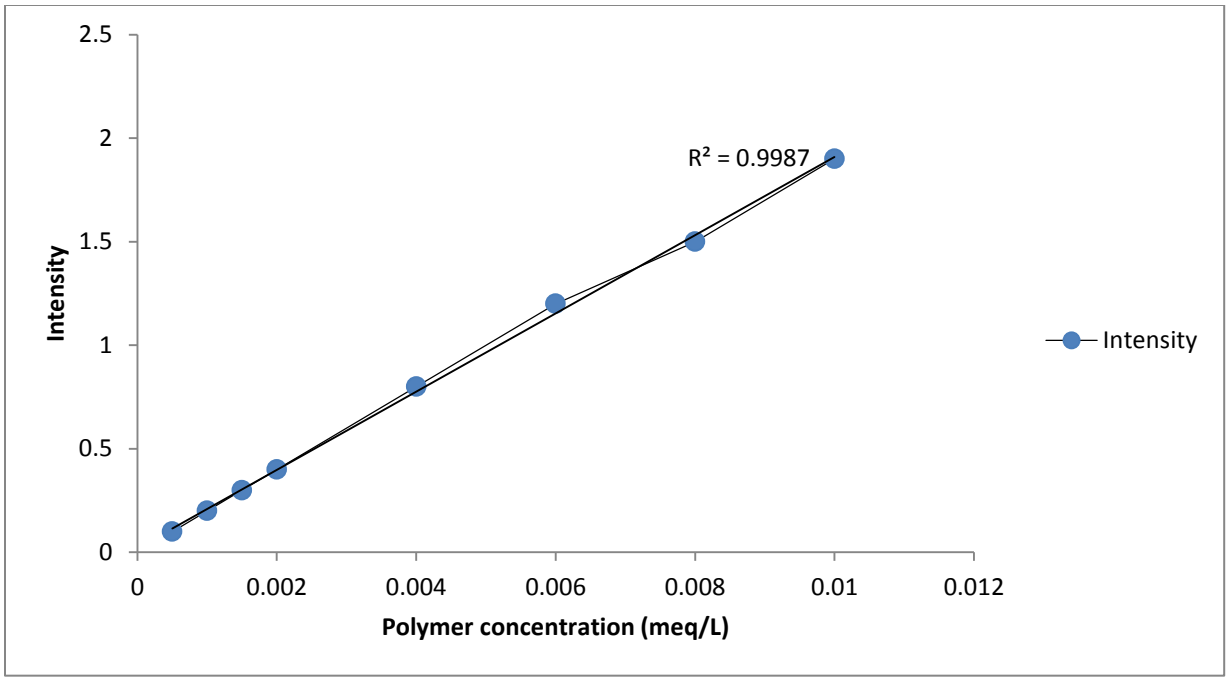

Figure A4. Standard Curve of fluorescence intensity vs concentration of PDADMAC-BCF

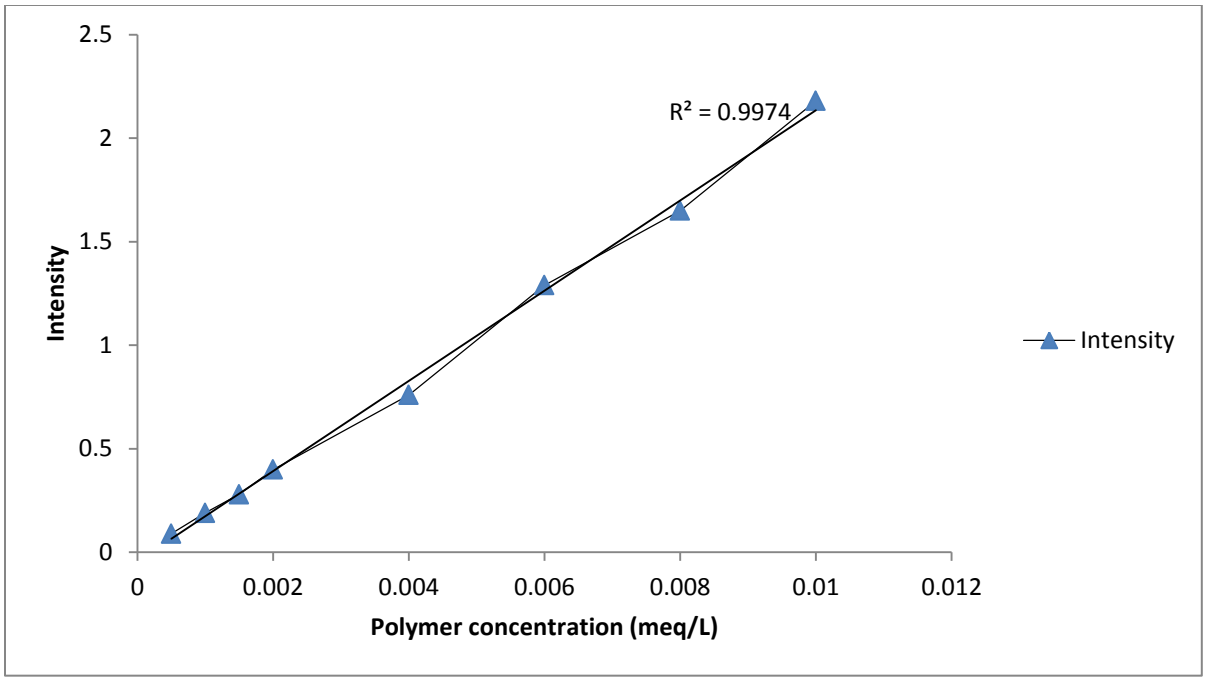

Figure A5. Standard Curve of fluorescence intensity vs concentration of PDADMAC-BC

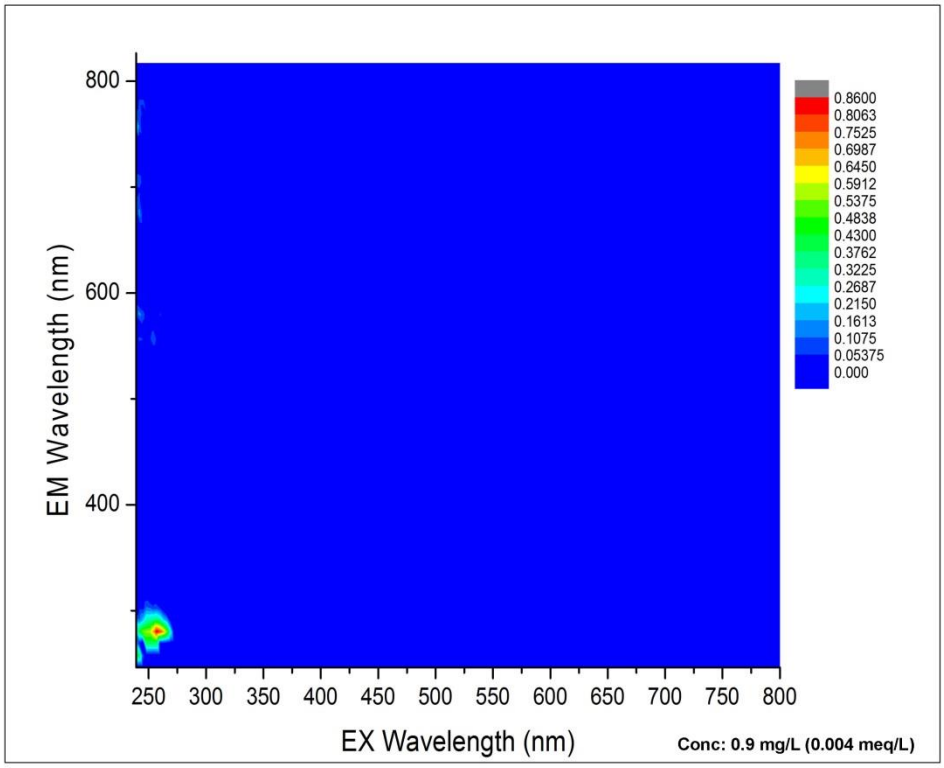

Figure A6. A sample standard fluorescence excitation emission matrix (F-EEM) obtained while testing PDADMAC-BCF in buffer used for preparing the DAF influent. Polymer peak excited and emitted at approximately 260 nm and 280 nm, respectively. Polymer concentration: 0.9 mg/L (0.004 meq/L)

Table A1. Polymers trialled: PDADMAC-BC, PDADMAC-BCF. Species trialled on: *Chlorella vulgaris* CS – 42/7 (Assays done in triplicate)

	Initial polymer concentration		**Residual polymer in treated effluent**		**% Polymer residual in treated effluent**
	meq/ L	**mg/L**	**meq/ L**	**mg/L**	
PDADMAC-BC	0.002	0.49	0.0012	0.303	62.3 ± 1.1
	0.004	0.98	0.00244	0.607	61.1 ± 1.9
	0.006	1.45	0.00372	0.899	62.2 ± 2.1
	0.008	2	0.0048	1.2	60.2 ± 1.6
	0.010	2.48	0.0055	1.364	55.6 ± 1.8
	Initial polymer concentration		**Residual polymer in treated effluent**		**% Polymer residual in treated effluent**
	meq/ L	**mg/L**	**meq/ L**	**mg/L**	
PDADMAC-BCF	0.002	0.45	0.00064	0.144	32.3 ± 2
	0.004	0.9	0.00132	0.297	33.4 ± 2.4
	0.006	1.4	0.00174	0.406	29.5 ± 0.8
	0.008	1.95	0.00184	0.448	23.2 ± 1.1
	0.010	2.45	0.0017	0.416	17.6 ± 1.7

Table A2. Polymers trialled: PDADMAC-BC, PDADMAC-BCF. Species trialled on: *Microcystis aeruginosa* CS – 564/01 (Assays done in triplicate)

	Initial polymer concentration		**Residual polymer in treated effluent**		**% Polymer residual in treated effluent**
	meq/ L	**mg/L**	**meq/ L**	**mg/L**	
PDADMAC-BC	0.0005	0.125	0.0003	0.303	60.3 ± 1.1
	0.001	0.25	0.0006	0.147	59.2 ± 1.9
	0.0015	0.375	0.00094	0.213	57.2 ± 2.1
	0.002	0.5	0.0013	0.305	61.2 ± 1.6
	0.0025	0.625	0.0014	0.412	66.6 ± 1.8
	Initial polymer concentration		**Residual polymer in treated effluent**		**% Polymer residual in treated effluent**
	meq/ L	**mg/L**	**meq/ L**	**mg/L**	
PDADMAC-BCF	0.0005	0.125	0.00064	0.041	33.3 ± 2
	0.001	0.25	0.00132	0.09	36.6 ± 2.4
	0.0015	0.375	0.00174	0.123	33.2 ± 0.8
	0.002	0.5	0.00184	0.08	16 ± 1.1
	0.0025	0.625	0.0017	0.143	23.3 ± 1.7

Table A3. Polymers trialled: PDADMAC-BC, PDADMAC-BCF. Species trialled on: *Microcystis aeruginosa* CS – 555/1 (Assays done in triplicate)

	Initial polymer concentration		**Residual polymer in treated effluent**		**% Polymer residual in treated effluent**
	meq/ L	**mg/L**	**meq/ L**	**mg/L**	
PDADMAC-BC	0.0005	0.125	0.00035	0.086	69 ± 16
	0.001	0.25	0.00078	0.195	78 ± 1.1
	0.0015	0.375	0.0012	0.28	75± 2.9
	0.002	0.5	0.0015	0.41	78 ± 2.1
	0.0025	0.625	0.0016	0.48	77 ± 2.5
	Initial polymer concentration		**Residual polymer in treated effluent**		**% Polymer residual in treated effluent**
	meq/ L	**mg/L**	**meq/ L**	**mg/L**	
PDADMAC-BCF	0.0005	0.125	0.00011	0.02	22 ± 3.6
	0.001	0.25	0.00029	0.07	29 ± 1.8
	0.0015	0.375	0.00042	0.106	28.5 ± 0.11
	0.002	0.5	0.00046	0.115	23 ± 2.8
	0.0025	0.625	0.00065	0.162	26 ± 3.3

Determining how polymer-bubble interactions impact algal separation using the novel "Posi"-dissolved air flotation process

Rao Hanumanth Rao, Narasinga

2018-03-06

Rao NR, Granville AM, Browne CI, Dagastine RR, Yap R, Jefferson B, Henderson RK, Determining how polymer-bubble interactions impact algal separation using the novel “Posi”-dissolved air flotation process, Separation and Purification Technology, Vol. 201, 7 August 2018, pp. 139-147

http://dx.doi.org/10.1016/j.seppur.2018.03.003